Journal Pre-proof

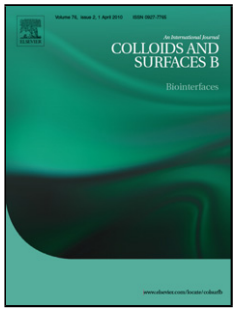

Inhibited enzymatic reaction of crosslinked lactate oxidase through a pH-dependent mechanism

Hugo Cunha-Silva, F. Pires, A.C. Dias-Cabral, M. Julia Arcos-Martinez

PII: S0927-7765(19)30634-4

DOI: https://doi.org/10.1016/j.colsurfb.2019.110490

Reference: COLSUB 110490

To appear in: *Colloids and Surfaces B: Biointerfaces*

Received Date: 28 May 2019

Revised Date: 12 August 2019

Accepted Date: 4 September 2019

Please cite this article as: Cunha-Silva H, Pires F, Dias-Cabral AC, Arcos-Martinez MJ, Inhibited enzymatic reaction of crosslinked lactate oxidase through a pH-dependent mechanism, *Colloids and Surfaces B: Biointerfaces* (2019), doi: https://doi.org/10.1016/j.colsurfb.2019.110490

Inhibited enzymatic reaction of crosslinked lactate oxidase through a pH-dependent mechanism

Hugo Cunha-Silva [a*], F. Pires [b,c], A. C. Dias-Cabral [b,c], M. Julia Arcos-Martinez [a]

[a]Departmento de Química, Facultad de Ciencias, Universidad de Burgos, Plaza Misael Bañuelos s/n, 09001 Burgos, Spain
[b]CICS-UBI – Health Sciences Research Centre, University of Beira Interior, 6200-506 Covilhã, Portugal
[c]Department of Chemistry, University of Beira Interior, 6200-001 Covilhã, Portugal

*e-mail: hfcunha@ubu.es

Graphical abstract

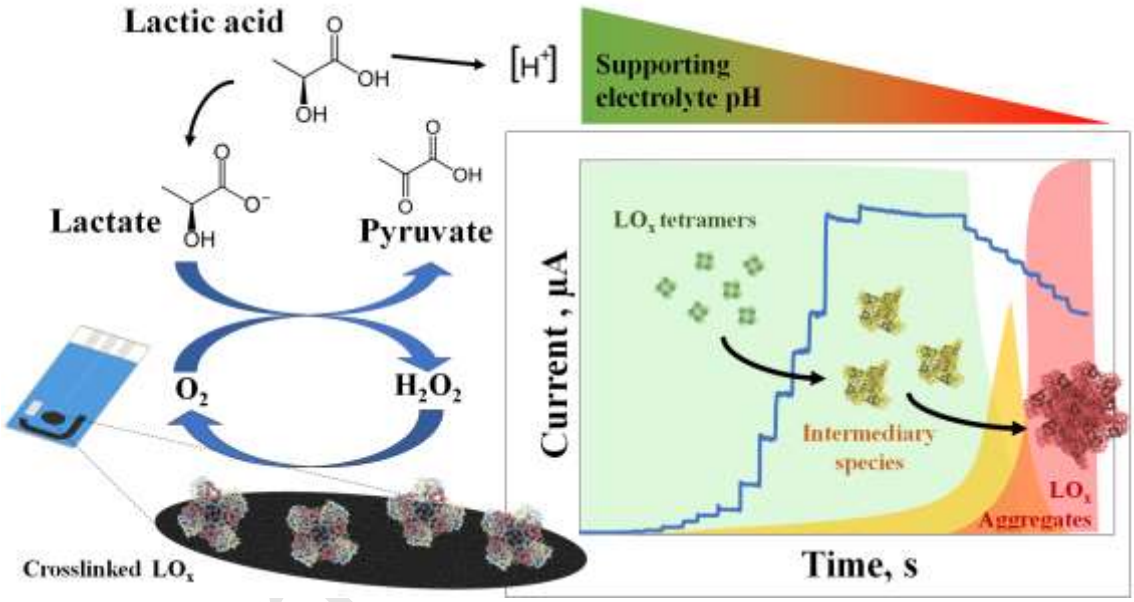

Highlights: "Inhibited enzymatic reaction of crosslinked lactate oxidase through a pH-dependent mechanism"

- Amperometric signal of crosslinked LO_x shows a substrate inhibition kinetics.
- Inhibition mechanism promotes conformational changes in LO_x structure.
- In solution, higher substrate concentration result in formation of LO_x aggregates.
- LO_x inhibition outcomes from a pH-dependent mechanism promoted by substrate.

Abstract

Lactate oxidase (LO_x), recognized to selectively catalyze the lactate oxidation in complex matrices, has been highlighted as preferable biorecognition element for the development of lactate biosensors. In a previous work, we have demonstrated that LO_x crosslinking on a modified screen-printed electrode results in a dual range lactate biosensor, with one of the analysis linear range (4 to 50 mM) compatible with lactate sweat levels. It was advanced that such behavior results from an atypical substrate inhibition process. To understand such inhibition phenomena, this work relies in the study of LO_x structure when submitted to increased substrate concentrations. The results found by fluorescence spectroscopy and dynamic light scattering of LO_x solutions, evidenced conformational changes of the enzyme, occurring in presence of inhibitory substrate concentrations. Therefore, the inhibition behavior found at the biosensor, is an outcome of LO_x structural alterations as result of a pH-dependent mechanism promoted at high substrate concentrations.

Keywords: Lactate oxidase inhibition; Amperometric biosensor; Lactic acid; Fluorescence spectrometry; Dynamic Light Scattering.

1. Introduction

Lactate, also known as lactic acid, is a valuable analyte with great interest in the analytical field. Lactate is the final product of glycolysis in many organisms, being of great interest in food industry where is used as freshness indicator for the quality and shelf-life stability of products [1]. It has been also used as acidulant and flavoring agent (E270), being of extreme importance its monitoring in the final products. Notwithstanding, the great demand for lactate analysis is found for the clinical and medical fields. As a critical metabolite of tissue oxygenation, lactate has been used as biomarker for different pathologies and as indicator for exercise prescription [2,3]. Lactate is produced from the anaerobic breakdown of glucose in the tissues aiming energy production, resulting in the biochemical process known as “lactic acidosis”. Whether from chronic dysfunction or

excessive production, high levels of this metabolite leads to a persistent oxygen debt and to the overwhelming of body's buffering abilities [2,3].

Lactate determination has been performed by means of several sensitive and accurate, but also, expensive, invasive and complicated techniques, unable to perform continuous monitoring [1]. Addressing a simple and low-cost analysis, several lactate biosensing approaches were released during the last decade [4–12]. In human body, this metabolite can be accessed through a non-invasive analysis of saliva [5,8,9,13] and sweat samples [6,13]. Especially attention has been given to sweat lactate, which concentration range usually relies between 3.7 mM and 50 mM, constituting on average 0.28% of sweat and contributing for its acidity [14].

Most of lactate biosensors are based on L-lactate oxidase enzyme (LO_x) (E.C.1.1.3.2.), a member of the α-hydroxyacid-oxidases flavoenzyme family. These proteins catalyze the flavin mononucleotide (FMN)-dependent oxidation of their respective substrates [15,16]. The enzymatic units are two tightly packed tetramers, each one forming a biologically active unit. Each monomer contains 15 α-helices, resulting in LO_x subunits folded in α/β-barrel with two short β-strands located at the bottom of the barrel, where is located the FMN-binding site of the active center [16]. This enzyme catalyzes the lactate oxidation using molecular oxygen to generate pyruvate and H_2O_2 , according to equation 1 [15–17].

$$L - lactate + O_2 \xrightarrow{LO_x} L - pyruvate + H_2O_2 \qquad (1)$$

This flavoprotein displays a high level of substrate specificity, discriminating lactate between foreign components present in several matrices. Lactate dehydrogenase (LDH), has been also used as biorecognition element in biosensing strategies, however, the requirement of the coenzymes NADH or NAD^+, prohibit a direct analysis of lactate, affecting the point-of-care commitment of such platforms. Also, the difficulty in immobilizing LDH on transducers surface, results in less selective and unstable devices [18]. These facts make of LO_x a preferable enzyme for biosensing technology.

Several LO_x-based electrochemical biosensing platforms are described in literature [4–6,8–13]. The majority of these works use screen-printed electrodes (SPEs) as transducers for biosensor fabrication, offering disposable, low-cost, easy-to-use, adaptable and point-of-care platforms, that are able to analyze very small volumes of usually untreated samples [19].

In a recent work, our group developed a LO_x-based screen-printed amperometric biosensor, that was successfully applied to the lactate analysis in samples of red and white wine, sweat and saliva [13]. This electrochemical approach, allowed to register the current generated from the oxidation of the enzymatically produced H_2O_2 (equation 2), and correlate it with the lactate concentration present in the problem samples.

$$H_2O_2 \xrightarrow{(+\,0.15\,V)} O_2 + 2H^+ + 2e^- \quad (2)$$

This amperometric biosensor was constructed by immobilizing the LO_x enzyme through a crosslinking assisted with a glutaraldehyde (GA), copper-metallic framework (Cu-MOF) and bovine serum albumin (BSA) on a working electrode modified with Pt. The biosensor's kinetic exhibited two linear ranges of analysis: a first catalytic zone up to 1 mM of lactate, which increased current signal reflects the catalysis described by equation 1; and the second linear range, from 4 to 50 mM, that shows a decrease in current signal due to a substrate-promoted inhibition process. Similar kinetic was found for three different LO_x types adsorbed onto working electrodes, confirming susceptibility of the biomolecule to this process [20].

Very few reports were found concerning LO_x inhibition. Some anions such as chloride, sulfate, nitrate, α-hydroxymalonate and high concentrations of phosphate are described as inhibitors of LO_x. In particular, phosphate anions are described to form reversible complexes with the enzyme competing with lactate and therefore, avoiding the flavin reduction for the catalytic cycle [21,22]. Also, biological components such as oxalate and hydrogencarbonate result in severe but transient inhibition of this biomolecule. Contrarily, phthalate shows an irreversible inhibition mechanism [22]. Molecules like 8-hydroxyquinoline, urea, ammonium, molybdate and uric acid, are also described to decrease LO_x activity [23]. Moreover, when used as enzymatic substrates lactate [13,20] and 2-hydroxy-3-butynoate [24,25] are described to result, respectively, in atypical kinetic of reversible and irreversible inhibitions.

In the present work, we explore the inhibition mechanism promoted by the substrate additions, considering the occurrence of conformational changes in LO_x structure. The decay in fluorescence intensity, indicates that inhibitory concentrations of lactate, outcome in conformational changes of the biomolecule. Also, the slightly acidic medium obtained in the inhibition experiments, evidenced the formation of LO_x aggregates by dynamic light scattering experiments. Gathering the structural data collected for the

enzyme solutions with the signal registered at the biosensor; a pH-dependent inhibition mechanism promoted by the high concentrations of substrate, is proposed for the crosslinked LO_x.

2. Materials and methods

2.1. Reagents and solutions

Lactate oxidase (LO_x) from *pediococcus sp.* (E.C. 1.1.3.2.) lyophilized powder (≥20 units/mg solid), chitosan, glutaraldehyde (GA), bovine serum albumin (BSA), terephthalic acid (1,4 – H_2BDC), triethylenediamine (TED) and N,N-Dimethylformamide (DMF), were purchased from Sigma-Aldrich (Steinheim, Germany). Potassium hexachloroplatinate (IV), potassium chloride, sodium phosphate dibasic dihydrate, sodium phosphate monobasic dihydrate and potassium chloride were obtained from Merck (Darmstadt, Germany). From Panreac-Applichem (Darmstadt, Germany) were purchased L-lactic acid (85%), sodium chloride and sodium hydroxide. Acetic acid from VWR (Briare, France).

The copper metal framework (Cu-MOF) was synthesized according to the previously reported method by [26] and [27]. Briefly, 100 mL of DMF were used to dissolved 0.493 g of copper nitrate trihydrate, 0.453 g of 1.4-H_2BDC and 0.320 g of TED. The mixture was sonicated to obtain a homogenous solution and heated at 120 ºC for 36 h. The obtained blue crystalline power was collected and after cooling at room temperature, washed with DMF and water several times. Finally, was dried under vacuum overnight.

All the reagents used were of analytical grade and Milli-Q water (Millipore, Bedford, USA) was employed for preparing all solutions.

In the fabrication of screen-printed electrodes, the inks used, namely Electrodag PF-407 A (carbon ink), Electrodag 6037 SS (silver/silver chloride ink), Electrodag 418 (silver ink) and Electrodag 452 SS (dielectric ink), were supplied by Achenson Colloiden (Scheemda, Netherlands). Polyester films (PET) of 0.5 mm thickness (HIFI Industrial Film, Dardily, France), were used as the printing substrates.

2.2. Screen-printed carbon electrodes (SPCE) manufacturing

A DEK 248 screen-printing system (DEK, Weymouth, UK) was used to fabricate SPCEs [28]. Using polyester screens with the appropriate stencil, the sequential deposition of the inks was performed to define the conductive silver tracks, the Ag/AgCl pseudo-reference electrode, the carbon counter electrode, the carbon working electrode (geometric area ~ 0.126 cm^2) and finally a dielectric layer.

2.3. SPCE modification for lactate biosensing

First, the carbon working electrode was modified with a Pt coating (Pt/SPCE). For that, cyclic voltammetric measurements were performed from 0.5 V to -0.7 V (vs SPE Ag/AgCl), with a scan rate of 0.002 V s^{-1}, using 200 µL drop of a 1 mM potassium hexachloroplatinate (IV) solution in 0.1 M KCl. After rinsed with Milli-Q water, the Pt modified working electrode was covered with 2.0 µL of 0.6 % chitosan (w/v) in 0.5 % acetic acid and dried at room temperature (CS/Pt/SPCE). Following, the enzyme was crosslinked onto the working electrode surface, by depositing 1.2 µL of a solution containing 3.0 µL of LO_x (1.5 U μL^{-1}, in 0.01 M phosphate buffer, pH 8.0), 3.0 µL of Cu-MOF (2 mg mL^{-1}), 0.56 µL of BSA (3 % (w/v)) and 0.56 µL of GA (2.5 % (v/v)). Finally, the LO_x – based biosensors (LO_x–Cu-MOF/CS/Pt/SPCE) were stored at 4 ºC in a refrigerator until use [13].

2.4. Electrochemical measurements

A PalmSens® portable electrochemical potentiostat with the PS Trace program (PalmSens® Instruments BV, Houten, The Netherlands) was used for chronoamperometric measurements of the biosensor modified with LO_x. The measurements were performed at room temperature in a cell containing 5.0 mL of supporting electrolyte, constituted by 0.1 M phosphate buffer (PB) at pH 7.0, and under constant stirring. The working electrode was operated at + 0.15 V (vs SPE Ag/AgCl), and after reaching a stable baseline, lactate concentrations were added to the electrochemical cell, from a stock solutions [13].

2.5. Fluorescence spectroscopic measurements

Fluorescence spectroscopic experiments were performed on a HITACHI F-7000 fluorescence spectrophotometer (Hitachi High-Tech, Tokyo, Japan), under excitation of λ_{exc} = 270 nm. Several LO_x solutions of 0.5 µg/µL, were prepared in 0, 2.0, 3.6, 10.0, 22.5, 35.0 and 47.5 mM of lactate and left at room temperature during 30 min. The spectra were registered with FL Solutions 4.0 Software for λ_{em} = 280 - 480 nm and using a quartz micro cell of 500 µL (10 x 2 mm) with an optical path length of 2 mm (Hellma Analytics, Müllheim, Germany). The signal noise was smoothed using 3-point Savitzky-Golay function.

2.6.Dynamic light scattering measurements

Dynamic light scattering (DLS) experiments were performed on a Malvern Zetasizer Nano-ZS system. Disposable polystyrene size cells for aqueous samples were used to carry the enzymatic reaction at 25 °C. For that, enzymatic, lactic acid and buffer solutions were previously filtered. The reaction was carried out for 0.25 U of LO_x in 40 µL of 0.1 M PB (pH 7.0), and L-lactic acid concentrations added to the cell and measured at each addition. A minimum of three measurements were made per sample.

3. Results and discussion

3.1. Determination of crosslinked LO_x kinetic parameters

The reaction rate for the crosslinked LO_x, is measured as a result of the H_2O_2 oxidation at + 0.15 V (vs SPE Ag/AgCl). The lactate additions to the electrochemical cell leads to the generation of higher amounts of this enzymatic product, consequently increasing the current intensity output.

Figure 1 displays the typical amperogram and the response current vs substrate concentration (*i vs [Lactate]*), which were used to construct lactate calibration curves for the biosensing analysis. As a result of the lactate concentrations present in the electrochemical cell, the LO_x exhibited two very distinct zones. The catalytic zone results from a first-order reaction, defined between 0 and 1 mM of lactate, in which the initial

rate depends linearly on the substrate concentration. After this zone, a current output stabilization was found until ~ 4 mM, reflecting a zero-order reaction; which was followed by a current signal decrease until 50 mM. This, second zone, revealed an inhibition phenomenon associated with the substrate, assuming a linearity applicable to samples with high content of this organic acid.

The application of kinetic models to determine the constants of immobilized bioreceptors, have been already used in biosensing field [20,29–31]. These models can be adapted for electrochemical signals, originating electrochemical equivalent equations. Regarding that the kinetic of crosslinked LO_x for the catalytic and inhibition zones, may be represented respectively by equations 3 and 4,

$$E + S \overset{K_M}{\longleftrightarrow} ES \rightarrow E + P \qquad (3)$$

$$ES + S \overset{K_I}{\longleftrightarrow} ESS \qquad (4)$$

with the definitions of $K_I = [S][ES]/[ESS]$ and $K_M = [S][E]/[ES]$, the assumption of rapid equilibrium yields:

$$i = \frac{i_{max}[S]}{K_M + [S] + \frac{[S]^2}{K_i}} \qquad (5)$$

where, *E* is the free enzyme, *S* the substrate, *ES* the enzyme-substrate complex, *P* the reaction products and K_M the Michaelis-Menten constant. *ESS* is the representation of an inactive complex, favored by the increment of *S* and K_I is the respective inhibition constant. *i* is the steady state current resulting from the substrate additions, i_{max} is the maximum current output registered for the saturation plateau, *[S]* the concentration of lactate [32].

A double-reciprocal plot describes the substrate inhibition kinetic (Figure S1 – B); therefore, parameters such as the Michaelis-Menten constant (K_M) for the catalytic range and the K_I value for the atypical uncompetitive substrate inhibition, can be obtained through the biosensor response. Moreover, the value of K_I was also used to determine the value of substrate concentration, after which the inhibition behavior initiates (S_{max}, substrate concentration resulting in the maximum reaction rate).

First, the current intensity values corresponding to the first-order kinetic and saturation zones (0 – 4 mM of lactate), were fitted to Lineweaver-Burk plot, using the

electrochemical equivalent equation 6 (Figure S1 – A), as under these conditions $[S]^2/K_i$ << 1, and inhibition effect is not observed:

$$\frac{1}{i} = \frac{1}{i_{max}} + \frac{K_M}{i_{max}}\frac{1}{[S]} \quad (6)$$

As shown in figure 2, the catalysis data fitted to equation 6 (*1/i = 0.0505 (1/[Lactate]) + 0.0426; R² = 0.9968*), resulted in the average values of 21.40 ± 1.84 µA for i_{max} and 1.05 ± 0.06 mM for K_M .The K_M value determined for the crosslinked enzyme, showed to be identical to the reported values of 0.87 mM [33] and 0.94 mM [17], both obtained for the free enzyme in buffered medium. Therefore, a similar intrinsic LO_x activity for lactate catalysis is attained, with the additional advantage of the biomolecule stabilization, which in turn, allows to achieve a stable and a reusable device for lactate determination.

Secondly, the inhibition noted at high substrate concentrations, resulted in alteration of the enzymatic activity, imposing changes in the kinetic values. High lactate concentrations promoted a decrease of the current signal, which is reflected in the increased significance of near zero values of the Lineweaver-Burk plot. As shown in equation 7, this contribution outcomes from the term $\frac{1}{i_{max}\,K_I}$, that gain importance in definition of the Lineweaver-Burk plots at substrate inhibition mechanisms (Figure S1 – B) [32].

$$\frac{1}{i} = \frac{K_M}{i_{max}}\frac{1}{[S]} + \frac{1}{i_{max}\,K_I}[S] \quad (7)$$

Under these conditions, the calculation of i_{max} and K_I values was carried out assuming a rapid equilibrium (Figure 3). At high lactate concentrations, those values can be determined by plotting *1/i* vs *[S]*, as defined in equation 8 (Figure S1 – C) [32].

$$\frac{1}{i} = \frac{1}{i_{max}} + \frac{[S]}{i_{max}\,K_I} \quad (8)$$

Using the interception value obtained from the curve of *1/i* vs *[S]* (*1/i = 0.0005 [Lactate] + 0.0406; R² = 0.9911*), an i_{max} of 24.94 ± 1.79 µA was obtained. This is in accordance with the values observed experimentally and with the one previously determined for the catalytic and saturation zones (21.40 ± 1.84 µA); further suggesting the evolvement of a substrate inhibition mechanism. Moreover, when the inhibition is dominant ([Lactate] >> K_M), a K_I value of 80.04 ± 19.61 mM was obtained from the curve slopes. To mention that LO_x activity is restored after each new experiment, exhibiting reversibility for the

substrate inhibition process, which contributes to the reusable character of the device. Nevertheless, after ten amperometric measurements, the sensitivity for lactate determinations started to decrease, indicating the occurrence of permanent effects [13]. Under repeated exposition to inhibitory conditions, irreversible conformational changes of the biomolecule structure, may be the cause for the consequent activity loss.

Finally, considering the previously determined kinetic parameters, it was possible to define the substrate concentration resulting in the maximum reaction rate, after which the inhibition process begins ($[S_{max}]$). Using equation 9, by setting $di/d[S] = 0$, a $[S_{max}]$ of 4.83 ± 0.30 mM was obtained (Figure S1 – D) [32].

$$[S_{max}] = \sqrt{K_M\, K_I} \quad (9)$$

This lactate concentration value agrees with the experimental data, where the current intensity output started to drop at values near to 4 mM of lactate. Thus, after the $[S_{max}]$ the crosslinked LO_x, developed a biosensing response based in inhibitory kinetics. In table 1, are summarized the kinetic constants, determined for the crosslinked LO_x at the different activity zones observed.

3.2. LO_x inhibition process

The biosensor response showed that the linearity observed up to 50 mM of lactate, gave place to a titration-like curve, when this concentration value was exceeded (Figure S2). This may be an indicator of an altered pH value, which in turn, may be related with the substrate concentration added to the supporting electrolyte. Lactate was added to the electrochemical cell from lactic acid stock solutions, which is easily dissociated in lactate and protons (pKa ~ 3.86) (Figure S3). Concerning this, in figure 4 are represented the current intensity values registered under a continuous pH monitoring, as function of the lactate concentrations. These plots showed that the current signal for the catalytic range (from 0 to 1 mM of lactate), increased under a stable pH of 7.0. At these conditions the previously determined K_M of 1.05 ± 0.06 mM, indicates an intrinsic LO_x activity. In contrast, the data obtained for saturation and inhibition zones, showed a decreased rate for lactate conversion, which can be related with the alteration of the pH value. The pH is decreased to values of 6.1, indicating that the crosslinked LO_x activity may be driven by the supporting electrolyte pH, rather than by an atypical substrate inhibition.

To confirm that no additional substrate inhibition is occurring, amperometric measurements were performed using more concentrated buffer solutions, such as 0.5 M and 1.0 M of phosphate buffer at pH 7.0 (Figure 5). Since the buffering capacity of a system depends on the concentration of its components, the increased amount of the acidic and basic phosphate salts, should improve the pH stabilization during the lactic acid additions. Therefore, using these buffered solutions, the LO_x catalytic activity should be isolated from the inhibition kinetic.

The amperometric signals registered for the substrate additions in strong buffer solutions, exhibited lower current intensities. This seems to be related with the LO_x inhibition promoted at high concentrations of phosphate anions [21]. Despite that, it is noticeable that the biosensor response displayed an extended saturation plateau, presenting stable current values until 50 mM of lactate, thus, avoiding the development of the inhibitory linear range. Considering that these solutions presented an increased buffer capacity, the LO_x inhibitory response observed in 0.1 M of phosphate buffer at pH 7.0, derives from the controlled perturbation of this buffer equilibrium, allowing to obtain a quantitative relation with the substrate added to the system. This characteristic is very significant, since it can be used to perform a biosensing analysis of samples containing high lactate concentrations. Therefore, to understand the behavior of the crosslinked biocatalyst in the inhibitory conditions, the influence of the substrate concentrations was studied regarding the LO_x structure when in solution.

3.3. LO_x structural changes promoted by substrate

It is well known that the charge of the biomolecules is dependent of the pH. An inadequate pH value can be usually associated with the decrease of the biological activity. Since the charges plays an important role maintaining the correct conformation of the enzymes, its alteration outcomes in conformational changes of the protein structure. These conformational alterations also affect the active center configuration, leading to the affinity loss for the substrates. Moreover, when the substrate present electric charges, its catalysis is also dependent of the active center residues charges, existing an equilibrium between pH value and the catalytic activity. Indeed, the majority of enzymes are recognized to have an optimal pH value, at which the formation of enzyme-substrate complex is favored and the catalytic activity is maximal [32].

Some mechanisms can occur after an alteration of the protein conformational state, occasionally resulting in the formation of protein aggregates, induced by partially unfolded intermediaries in solution. Moreover, the changes in protein structure, can also result in the biomolecule adsorption to solid-liquid interfaces [34].

Considering the influence of pH value in proteins structure and the overall data presented, LO_x solutions were studied by fluorescence spectroscopy to explore changes in the biomolecule conformational state, and the results associated with the amperometric signal registered for the crosslinked LO_x.

3.3.1. Fluorescence spectroscopy

LO_x is a particular case of intrinsic fluorescence associated with the reduced form of FMN in the biomolecule structure. The reduced FMN presents higher fluorescence than the oxidized form, being suitable to access the kinetic of lactate metabolization [35,36]. However, LO_x structure holds aromatic amino acid residues, such as tryptophan (Trp) and tyrosine (Tyr), that can be also probed using intrinsic fluorescence. Such residues can be easily related with the conformational state of the biomolecule, being preferable in structural studies. This polypeptide contain respectively, five and sixteen residues of Trp and Tyr [37]. Such residues are generally located within the hydrophobic core of the protein, presenting a high quantum yield and therefore, a high fluorescence intensity. In contrast, in presence of a hydrophilic environment the fluorescence intensity for these residues is decreased. Thus, the fluorescence emission spectra of a protein, reflect changes in the environment of the aromatic amino acids residues, indicating a tertiary structure alteration due to improper folding; being consequently associated with the activity loss of the enzymes [38,39]. To inspect the inactivation behavior promoted at inhibitory concentrations of lactate, the LO_x intrinsic fluorescence spectra was evaluated under increased concentrations of this substrate.

As shown in figure 6, the fluorescence emission spectra of LO_x after excitation at a λ_{exc} = 270 nm, presents a decreased fluorescence intensity (λ_{em} =330 nm) at higher substrate concentrations. The fluorescence recorded for the enzyme solutions in absence of lactate, was considered the one associated with the full active LO_x structures, giving a fluorescence intensity value of 914.6 ± 19.4. Moreover, between 2.0 and 3.6 mM of

lactate, the LO_x solutions exhibited respectively, 94.08 % and 92.40 % of the native structure fluorescence. Comparing these data with the signal registered at the biosensor during the saturation plateau, the high fluorescence values reveal an active and correct conformational state of the biocatalyst. In fact, LO_x displayed the maximum catalysis rate, generating the maximal current signal obtained in the biosensor analysis.

On the other hand, contrasting information was found for the fluorescence data in the inhibitory lactate levels. In presence of lactate at 10.0 mM, a fluorescence intensity value of 759.9 ± 25.7 was observed, evidencing the presence of biomolecules with about 20 % less fluorescence. Thus, the slightly acidic conditions reached in presence of high substrate concentrations, led to alterations on the enzymatic core environment, and consequently, resulted in changes of the biomolecule conformational state. Furthermore, regarding the amperometric response registered for 10.0 mM of lactate, it is possible to associate the decreased enzymatic activity with the conformational changes detected in fluorescence experiments.

Lactate concentrations higher than 10.0 mM, presented a slower decay of the fluorescence values of the LO_x solutions; however, displayed a strong inhibition in the amperometric response. This indicate that, after this point, different processes are occurring at the LO_x structural conformation. Therefore, there is the possibility that the immobilized enzyme is undergoing conformational changes at the electrode surface, resulting in the inhibitory zone observed. The nearly steady state of fluorescence observed after 10.0 mM, specify that the surrounding environment of the aromatic aminoacidic residues does not undergo in extensive modifications. Accordingly, these data point to the formation of aggregates, in which the hydrophobic residues are usually present in the interior of these structures. Thus, dynamic light scattering (DLS) of LO_x solutions was used to evaluate and identify the formation of protein aggregates in inhibitory conditions.

3.3.2. Dynamic light scattering

Dynamic light scattering (DLS) is a well-established and widely used tool, to evaluate hydrodynamic size and size distribution of several type of particles such as proteins, protein aggregates, polymers or nanoparticles. Based on the scattering of light from particles and their Brownian motion, this technique allows to determine a broad range of hydrodynamic sizes [40]. The destabilization and unfolding phenomena of proteins

typically result in the displaying of aminoacidic residues that create nucleation points for aggregates growth. These aggregates, generally show a lack of catalytic activity and can be formed from a combination of hydrophobic interactions, hydrogens bonds and/or Van der Waals forces [34], all favored with changes on the medium pH. Accordingly, it is possible to identify such aggregates through the increase of the hydrodynamic size of species in solution (Figure S4).

DLS experiments were carried out in LO_x and 0.1 M PB (pH 7.0) solutions, and the size distribution evaluated under different lactate concentrations. In absence of substrate, it was found a monodisperse solution; however, the polydispersity started to be evident when lactate was added to the medium. This polydispersity is associated with the presence of a nonpure hydrodynamic size distribution, therefore, indicating the presence of different sizes in solution.

Relying in distribution, the DLS data were collected into three main hydrodynamic size families: the smallest size of 8.99 ± 0.55 nm (Family 1); an intermediary size of 56.64 ± 12.43 nm (Family 2), and finally, with a size of 263.63 ± 23.90 nm the larger particles (Family 3). This size distribution can be related with LO_x aggregation, as a result of the alteration in solution properties during lactate additions.

Estimated with a molecular weight of 80 kDa, the smallest particles of family 1 are representative of non-aggregated and full active LO_x structures, which displays the same molecular weight in gel filtration. As can be seen in figure 7, the presence of this hydrodynamic size prevailed between 0 and 3.6 mM of lactate, after which the percentage started to decrease, marking the beginning of the inhibition zone observed for the crosslinked enzyme. The homogeneous distribution of the family 1 during the catalytic and saturation zones, showed that the major contribution for the electrochemical signal generation, is due to the native structures of LO_x, which offer intrinsic activity for lactate conversion.

Despite the prevalence of these active structures during the catalytic and saturation zones, the presence of intermediary species (Family 2), was noticeable since the beginning of substrate additions. The size distribution of family 2, remained lower than 0.2 % during the catalytic and saturation zones of the amperometric response, contributing to the polydispersity of the solution. The presence of this family showed insignificant effects on the global activity registered in the catalytic and saturation zones for the crosslinked LO_x.

The homogeneity of sizes distribution suffered a drastic change in lactate range from 3.6 and 22.5 mM. For 10.0 mM of lactate, the family 1 distribution dropped to 98.8%, the family 2 was kept at 0.2 %, and a new family 3 of larger hydrodynamic sizes appeared in solution. The presence of the family 3 confirmed, that the native structures of LO_x are aggregating, due to the destabilization of the medium pH. At 22.5 mM of lactate, the solutions' size distribution was completely changed, with only 34 % of family 1, also showing an increased presence of family 2 intermediary species (65 %) and nearly 0.5 % of family 3 prevalence. The family 2, with the intermediary structures, played an important role in the aggregation mechanism, acting like a trigger for the formation of larger and inactive protein aggregates. At this point, the decrease in amperometric signal, can be associated with the low availability of active and non-aggregated LO_x structures that, in solution, have been mainly converted into larger and inactive aggregates. Indeed, at higher substrate concentrations, the family 3 prevailed as the main species in solution. DLS experiments, also indicate that, the native LO_x structures and the intermediary species of family 2, were totally depleted at the highest substrate concentrations tested. In fact, a monodisperse solution of larger LO_x aggregates was noticed.

Gathering the DLS and amperometric results with the fluorescence data, it is possible to associate the fluorescence intensity decay, observed between 10.0 and 47.5 mM of lactate, with the formation of the larger LO_x sizes from family 3 (Figure 7). These aggregates internalize the hydrophobic residues, stabilizing the fluorescence intensity values. Moreover, concerning this effect, the inhibited enzymatic reaction of crosslinked LO_x reflect conformational changes on the tertiary structure of the immobilized protein, that present a decreased affinity to the substrate, due to a pH-dependent mechanism.

4. Conclusions

The results obtained in this work explore the substrate inhibition mechanism detected for the crosslinked LO_x. Conformational alterations of the enzyme structure in solution were accompanied during the course of the catalytic and inhibitory reactions.

Throughout the analysis performed with the biosensor, it was found that substrate additions to the electrochemical cell, resulted in slightly acidic supporting electrolyte. The change in the supporting electrolyte buffering equilibrium, affected the crosslinked LO_x activity, giving place to lower rates for substrate catalysis. The use of concentrated

phosphate buffer solutions as supporting electrolyte in amperometric measurements, allowed to observe an enzymatic saturation extended up to 50 mM, demonstrating that such inhibition mechanism was related with a pH variation, rather than with a substrate inhibition.

The decay in LO_x intrinsic fluorescence intensity, evidenced conformational alterations on the enzyme tertiary structure, with dependence of substrate concentrations. Moreover, the presence of a fluorescence steady state for inhibitory zone, indicated the internalization of hydrophobic residues into different protein structures. Moreover, the DLS data, showed that the hydrodynamic size detected in LO_x solutions, was also highly dependent of lactate concentrations. For the catalytic range (0 – 1 mM of lactate), the enzymatic solutions evidenced the native form of LO_x. However, during the saturation zone the availability of non-aggregated LO_x structures started to drop, giving place to intermediary species. These intermediaries, were noted as transitional stages for the nucleation into larger aggregates, demonstrating its importance in the aggregation mechanism in solution. In fact, substrate concentrations that exhibit a stronger inhibition, resulted in the formation of larger and inactive LO_x aggregates, which constitute 100% of the solution hydrodynamic size distribution.

Accordingly, it was possible to establish a relation between the conformational changes and the consequent aggregation of the enzyme in solution, with the supporting electrolyte pH, perturbed by the substrate additions. Therefore, these factors are the main contributors in the crosslinked LO_x activity loss, and consequently, the main cause for inhibitory range observed in the biosensing approach.

5. Acknowledgements

This work was supported by the Spanish Ministry of Science and Innovation (MICINN), Ministry of Economy and Competitiveness (MINECO) and the European Regional Development Fund (FEDER) (TEC20013-40561-P and MUSSEL RTC-2015-4077-2). Hugo Cunha-Silva would like to acknowledge funding from the Spanish Ministry of Economy (BES-2014-068214).

6. Bibliography

[1] K. Rathee, V. Dhull, R. Dhull, S. Singh, Biosensors based on electrochemical lactate detection: A comprehensive review, Biochem. Biophys. Reports. 5 (2016) 35–54. doi:10.1016/j.bbrep.2015.11.010.

[2] L.B. Gladden, Lactate metabolism: A new paradigm for the third millennium, J Physiol. 558 (2004) 5–30. doi:10.1113/jphysiol.2003.058701.

[3] N. Nikolaus, B. Strehlitz, Amperometric lactate biosensors and their application in (sports) medicine, for life quality and wellbeing, Microchim. Acta. 160 (2008) 15–55. doi:10.1007/s00604-007-0834-8.

[4] P. Giménez-Gómez, M. Gutiérrez-Capitán, F. Capdevila, A. Puig-Pujol, C. Fernández-Sánchez, C. Jiménez-Jorquera, Monitoring of malolactic fermentation in wine using an electrochemical bienzymatic biosensor for l-lactate with long term stability, Anal. Chim. Acta. 905 (2016) 126–133. doi:10.1016/j.aca.2015.11.032.

[5] J. Kim, G. Valdés-Ramírez, A.J. Bandodkar, W. Jia, A.G. Martinez, J. Ramírez, P. Mercier, J. Wang, Non-invasive mouthguard biosensor for continuous salivary monitoring of metabolites, Analyst. 139 (2014) 1632–6. doi:10.1039/c3an02359a.

[6] W. Gao, S. Emaminejad, H.Y.Y. Nyein, S. Challa, K. Chen, A. Peck, H.M. Fahad, H. Ota, H. Shiraki, D. Kiriya, D.-H. Lien, G.A. Brooks, R.W. Davis, A. Javey, Fully integrated wearable sensor arrays for multiplexed in situ perspiration analysis, Nature. 529 (2016) 509–514. doi:10.1038/nature16521.

[7] M.J. Arcos-Martínez, H. Cunha-Silva, J. Sedano Franco, A. Navarro Benito, M. Porta García, Dispositivo electródico y procedimiento de medida para la detección de ácido láctico, 2638737, 2018.

[8] J. Ballesta Claver, M.C. Valencia Mirón, L.F. Capitán-Vallvey, Disposable electrochemiluminescent biosensor for lactate determination in saliva, Analyst. 134 (2009) 1423–32. doi:10.1039/b821922b.

[9] K. Petropoulos, S. Piermarini, S. Bernardini, G. Palleschi, D. Moscone, Development of a disposable biosensor for lactate monitoring in saliva, Sensors Actuators, B Chem. 237 (2016) 8–15. doi:10.1016/j.snb.2016.06.068.

[10] R. Monošík, M. Streďanský, G. Greif, E. Šturdík, A rapid method for

determination of l-lactic acid in real samples by amperometric biosensor utilizing nanocomposite, Food Control. 23 (2012) 238–244. doi:10.1016/j.foodcont.2011.07.021.

[11] S. Anastasova, B. Crewther, P. Bembnowicz, V. Curto, H.M. Ip, B. Rosa, G.Z. Yang, A wearable multisensing patch for continuous sweat monitoring, Biosens. Bioelectron. 94 (2017) 730. doi:10.1016/j.bios.2017.03.018.

[12] I.S.S. Kucherenko, Y.V. V. Topolnikova, O.O.O. Soldatkin, Advances in the biosensors for lactate and pyruvate detection for medical applications: a review, TrAC Trends Anal. Chem. 110 (2018) 160–172. doi:10.1016/J.TRAC.2018.11.004.

[13] H. Cunha-Silva, M.J. Arcos-Martinez, Dual range lactate oxidase-based screen printed amperometric biosensor for analysis of lactate in diversified samples, Talanta. 188 (2018) 779–787. doi:10.1016/j.talanta.2018.06.054.

[14] A.B. Stefaniak, C.J. Harvey, Dissolution of materials in artificial skin surface film liquids, Toxicol. Vitr. 20 (2006) 1265–1283. doi:10.1016/j.tiv.2006.05.011.

[15] Y. Umena, K. Yorita, T. Matsuoka, A. Kita, K. Fukui, Y. Morimoto, The crystal structure of l-lactate oxidase from Aerococcus viridans at 2.1 Å resolution reveals the mechanism of strict substrate recognition, Biochem. Biophys. Res. Commun. 350 (2006) 249–256. doi:10.1016/j.bbrc.2006.09.025.

[16] I. Leiros, E. Wang, T. Rasmussen, E. Oksanen, H. Repo, S.B. Petersen, P. Heikinheimo, E. Hough, The 2.1 Å structure of Aerococcus viridans L-lactate oxidase (LOX), Acta Crystallogr. Sect. F Struct. Biol. Cryst. Commun. 62 (2006) 1185–1190. doi:10.1107/S1744309106044678.

[17] K. Maeda-Yorita, K. Aki, H. Sagaib, H. Misakib, V. Massey, L-Lactate oxidase and L-lactate monooxygenase : Mechanistic variations on a common structural theme, Biochimie. 77 (1995) 631–642.

[18] C.S. Pundir, V. Narwal, B. Batra, Determination of lactic acid with special emphasis on biosensing methods: A review, Biosens. Bioelectron. 86 (2016) 777–790. doi:10.1016/j.bios.2016.07.076.

[19] O.D. Renedo, M.A. Alonso-Lomillo, M.J.A. Martínez, Recent developments in the

field of screen-printed electrodes and their related applications., Talanta. 73 (2007) 202–19. doi:10.1016/j.talanta.2007.03.050.

[20] I. Taurino, R. Reiss, M. Richter, M. Fairhead, L. Thöny-Meyer, G. De Micheli, S. Carrara, Comparative study of three lactate oxidases from Aerococcus viridans for biosensing applications, Electrochim. Acta. 93 (2013) 72–79. doi:10.1016/j.electacta.2013.01.080.

[21] O. Lockridge, V. Massey, P.A. Sullivan, Mechanism of action in the flavoenyzme lactate oxidase, J. Biol. Chem. 247 (1972) 8097–8106.

[22] M. Mascini, D. Moscone, G. Palleschi, A lactate electrode with lactate oxidase immobilized on nylon net for blood serum samples in flow systems, Anal. Chim. Acta. 157 (1984) 45–51. doi:10.1016/S0003-2670(00)83604-1.

[23] S. Suman, R. Singhal, A.L. Sharma, B.D. Malthotra, C.S. Pundir, Development of a lactate biosensor based on conducting copolymer bound lactate oxidase, Sensors Actuators, B Chem. 107 (2005) 768–772. doi:10.1016/j.snb.2004.12.016.

[24] C.T. Walsh, A. Schonbrunn, O. Lockridge, V. Massey, R. H. Abeles, Inactivation of a Flavoprotein, Lactate Oxidase, by Acetylenic Substrate, J. Biol. Chem. 247 (1972) 6004–6006.

[25] S. Ghisla, V. Massey, R.H. Abeles, C.T. Walsh, H. Ogata, A. Schonbrunn, Kinetic Studies on the Inactivation of L-Lactate Oxidase by [the Acetylenic Suicide Substrate]2-Hydroxy-3-Butynoate, Biochemistry. 15 (1976) 1791–1797. doi:10.1021/bi00654a002.

[26] J.Y. Lee, D.H. Olson, L. Pan, T.J. Emge, J. Li, Microporous metal-organic frameworks with high gas sorption and separation capacity, Adv. Funct. Mater. 17 (2007) 1255–1262. doi:10.1002/adfm.200600944.

[27] X. Wang, X. Lu, L. Wu, J. Chen, 3D metal-organic framework as highly efficient biosensing platform for ultrasensitive and rapid detection of bisphenol A, Biosens. Bioelectron. 65 (2015) 295–301. doi:10.1016/j.bios.2014.10.010.

[28] B. Molinero-Abad, D. Izquierdo, L. Pérez, I. Escudero, M.J. Arcos-Martínez, Comparison of backing materials of screen printed electrochemical sensors for direct determination of the sub-nanomolar concentration of lead in seawater,

Talanta. 182 (2018) 549–557. doi:10.1016/j.talanta.2018.02.005.

[29] R. Baronas, J. Kulys, A. Lančinskas, A. Žilinskas, Effect of diffusion limitations on multianalyte determination from biased biosensor response, Sensors (Switzerland). 14 (2014) 4634–4656. doi:10.3390/s140304634.

[30] J. Kulys, Biosensor Response at Mixed Enzyme Kinetics and External Diffusion Limitation in Case of Substrate Inhibition, Nonlinear Anal. Model. Control. 11 (2006) 385–392.

[31] D. Simelevicius, R. Baronas, Mechanisms controlling the sensitivity of amperometric biosensors in flow injection analysis systems, J. Math. Chem. 49 (2011) 1521–1534. doi:10.1007/s10910-011-9838-z.

[32] M.L. Shuler, F. Kargi, Enzymes, in: Bioprocess Eng. - Basic Concepts, 2nd ed., Upper Saddle River, NJ : Prentice Hall, 2002: pp. 57–97. doi:10.1016/0168-3659(92)90106-2.

[33] K. Yorita, K. Aki, T. Ohkuma-Soyejima, T. Kokubo, H. Misaki, V. Massey, Conversion of L-lactate oxidase to a long chain α-hydroxyacid oxidase by site-directed mutagenesis of alanine 95 to glycine, J. Biol. Chem. 271 (1996) 28300–28305. doi:10.1074/jbc.271.45.28300.

[34] W. Wang, C.J. Roberts, Protein aggregation – Mechanisms, detection, and control, Int. J. Pharm. 550 (2018) 251–268. doi:10.1016/j.ijpharm.2018.08.043.

[35] J. Galbán, I. Sanz-Vicente, J. Navarro, S. De Marcos, The intrinsic fluorescence of FAD and its application in analytical chemistry: A review, Methods Appl. Fluoresc. 4 (2016). doi:10.1088/2050-6120/4/4/042005.

[36] W. Trettnak, O.S. Wolfbeis, A fully reversible fiber optic lactate biosensor based on the intrinsic fluorescence of lactate monooxygenaseVollreversibler faseroptischer Lactatbiosensor aufgrund der Eigenfluorescenz der Lactatmonooxygenase, Fresenius' Zeitschrift Für Anal. Chemie. 334 (1989) 427–430. doi:10.1007/bf00469465.

[37] H. Minagawa, N. Nakayama, S. Nakamoto, Thermostabilization of lactate oxidase by random mutagenesis, Biotechnol. Lett. 17 (1995) 975–980. doi:10.1007/BF00127437.

[38] M.R. Eftink, Fluorescence Techniques for Studying Protein Structure, 1991. doi:10.1002/9780470110560.ch3.

[39] B. Manta, G. Obal, A. Ricciardi, O. Pritsch, A. Denicola, Tools to evaluate the conformation of protein products, Biotechnol. J. 6 (2011) 731–741. doi:10.1002/biot.201100107.

[40] A. Khodabandehloo, D.D.Y. Chen, Particle sizing methods for the detection of protein aggregates in biopharmaceuticals, Bioanalysis. 9 (2017) 313–326. doi:10.4155/bio-2016-0269.

Figure Captions:

Figure 1. Electrochemical response of LO_x–Cu-MOF/CS/Pt/SPCE biosensor. (A) Amperogram registered at + 0.15 V (vs SPE Ag/AgCl) for successive additions of lactate in PB (0.1 M, pH 7.0); and (B) Plotting of current vs lactate concentration (n=5). Inset: calibration curve for lactate concentration range from 0 to 1.0 mM.

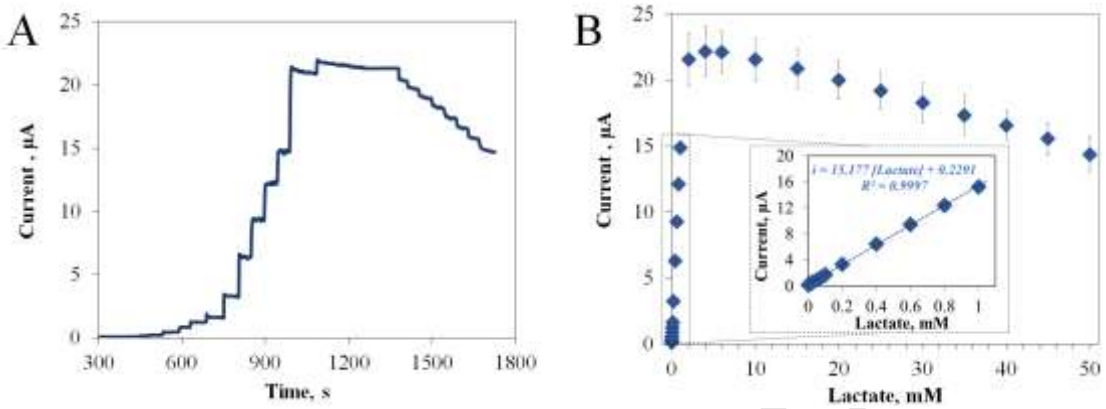

Figure 2. Determination of the crosslinked LO_x kinetic constants. Lineweaver-Burk model fitting to the catalytic range using the amperometric response for lactate additions at 0.1 M PB, pH 7.0 (n=5).

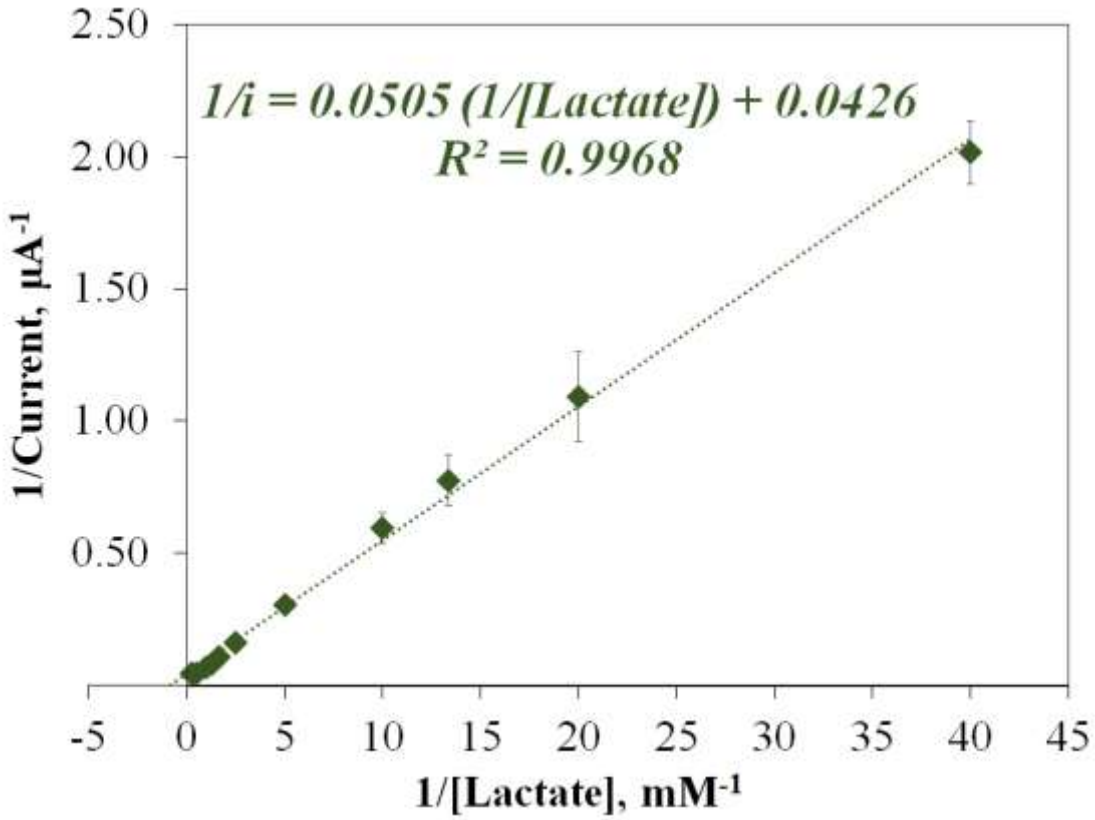

Figure 3. Determination of the crosslinked LO_x kinetic parameters in inhibition range assuming a rapid equilibrium. Representation of 1/i vs [S], in lactate additions at PB (0.1 M, pH 7.0) (n=5).

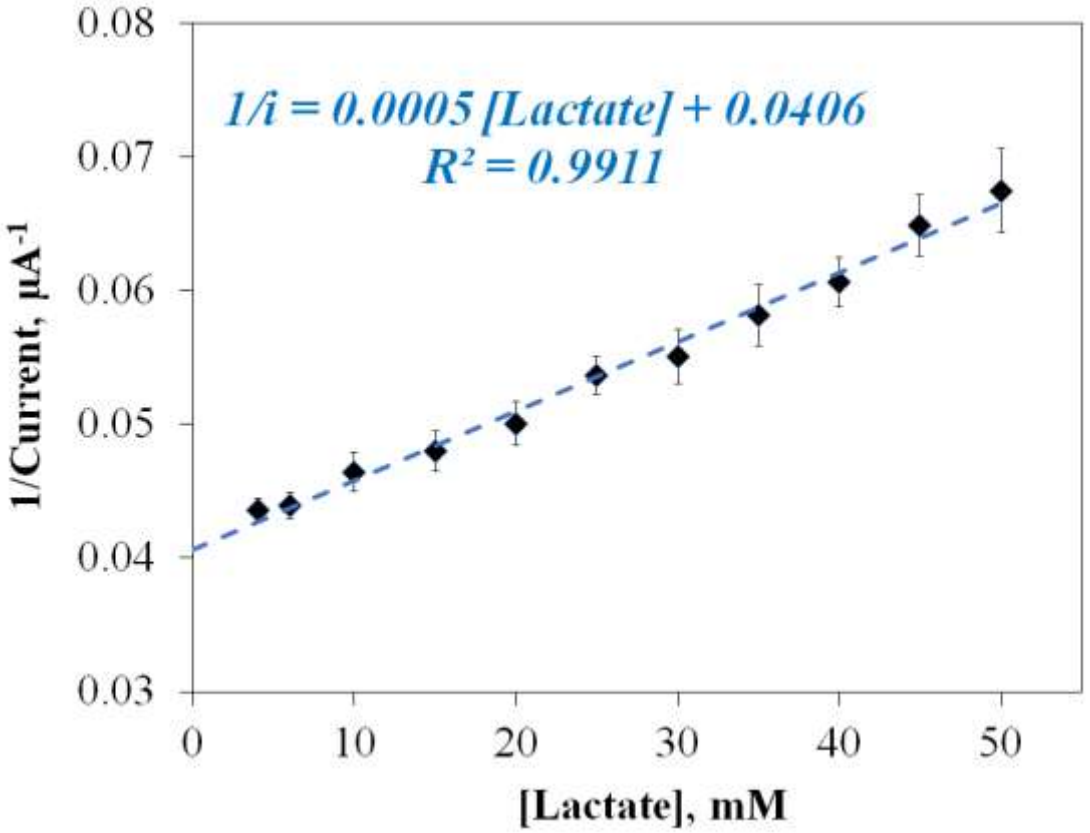

Figure 4. LO_x–Cu-MOF/CS/Pt/SPCE biosensor kinetic registered at + 0.15 V (vs SPE Ag/AgCl) and pH variation with lactate concentration in supporting electrolyte (0.1 M PB at pH 7.0).

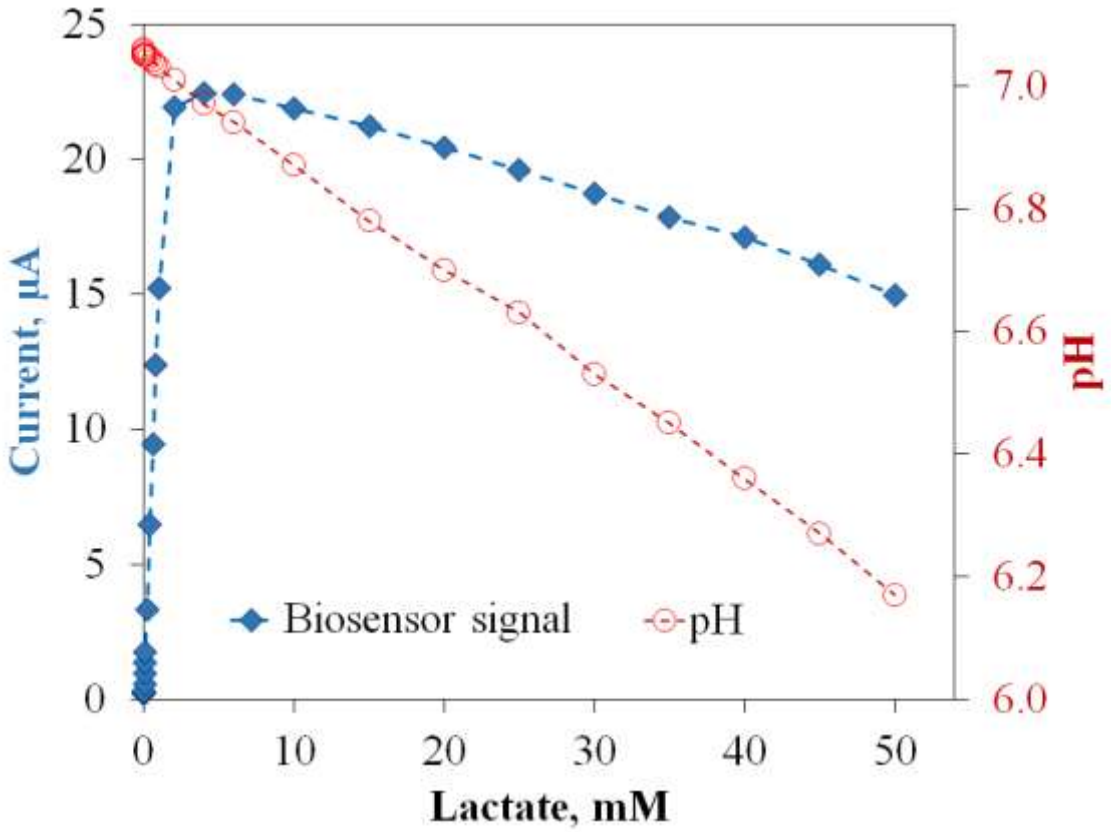

Figure 5. Influence of phosphate buffer concentration in the amperometric signal. (A) Current registered at + 0.15 V (vs Ag/AgCl), using the LO_x–Cu-MOF/CS/Pt/SPCE biosensor; (B) Variation of the calibration curves' slope with the phosphate concentration in supporting electrolyte.

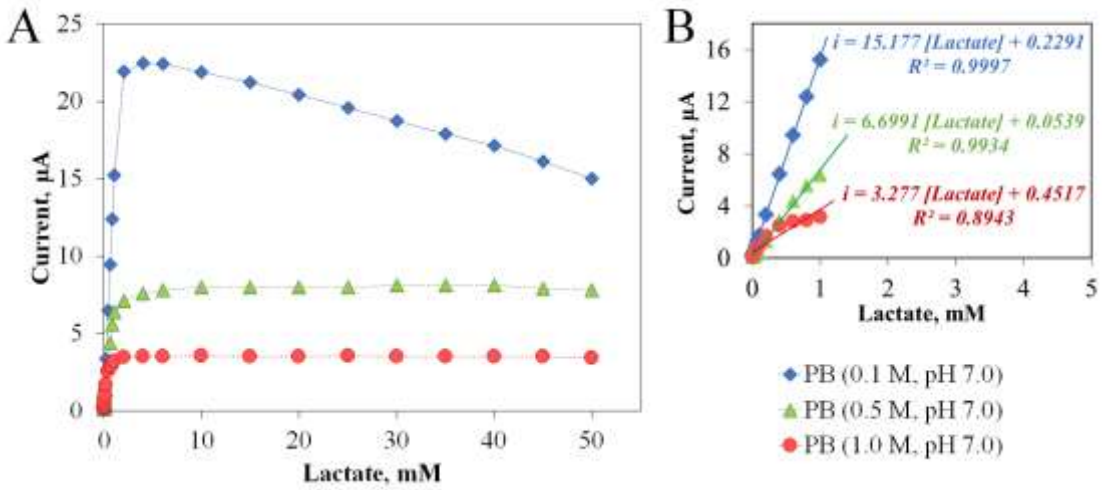

Fig. 6. Fluorescence spectroscopy for LO_x solutions. (A) Fluorescence spectra of LO_x (0.5 µg/µL) in 0.1 M PB (pH 7.0), containing 0, 2.0, 3.6, 10.0, 22.5, 35.0 and 47.5 mM of lactate (λ_{exc} = 270 nm); (B) LO_x conformational changes monitored by collecting the fluorescence intensity at 330 nm for increased lactate concentrations (n=3).

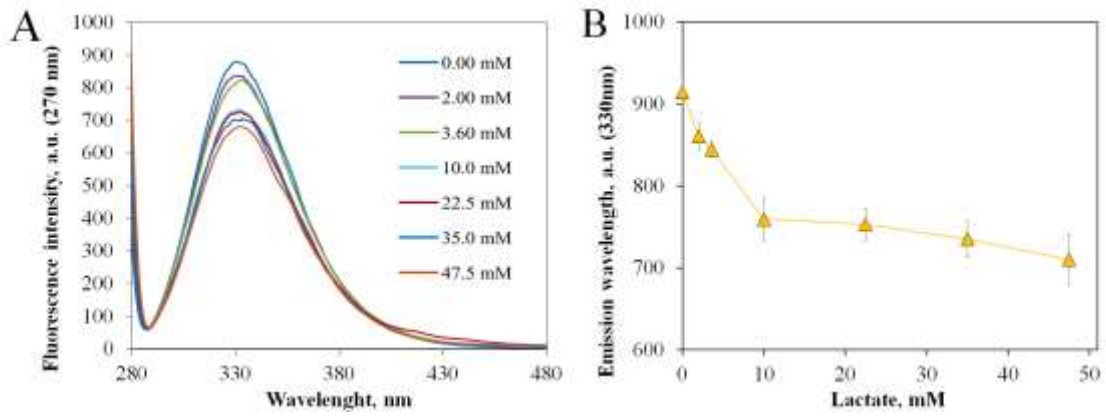

Figure 7. DLS analysis. Hydrodynamic size distribution by volume for LO_x solutions in presence of different lactate concentrations (0.1 M PB, pH 7.0). Data obtained from the distribution results.

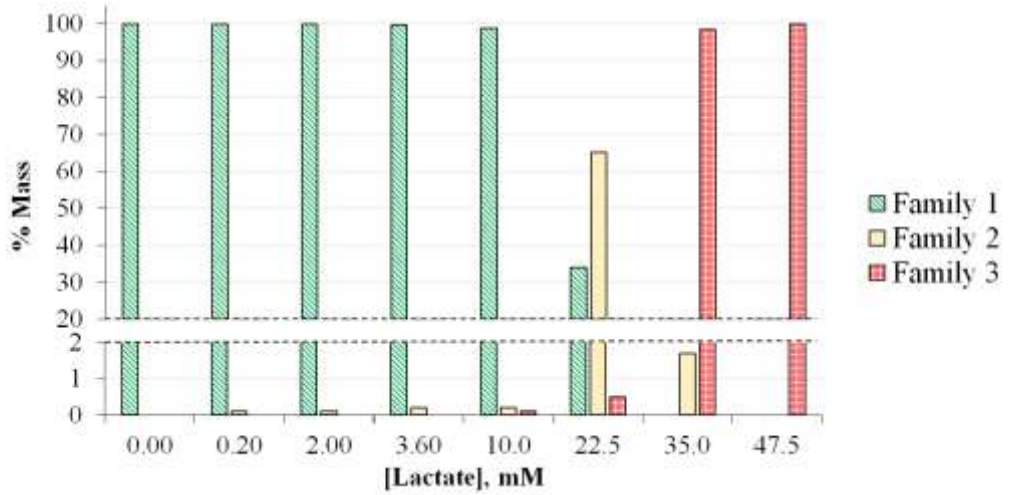

Tables and captions:

Table 1. Kinetic parameters obtained for LO_x in normal catalysis and in the atypical substrate inhibition obtained with the biosensor (n=5).

Lactate Oxidase	Catalytic Kinetic	Inhibition Kinetic
Crosslinked	i_{max} = 21.40 ± 1.84 µA K_M = 1.05 ± 0.06 mM	i_{max} = 24.94 ± 1.79 µA K_I = 80.04 ± 19.61 mM $[S_{max}]$= 4.83 ± 0.30 mM